A Mean-Field Theory for Coarsening Faceted Surfaces

Scott A. Norris and Stephen J. Watson

July 5, 2021

Abstract

A mean-field theory is developed for the scale-invariant length distributions observed during the coarsening of generic one-dimensional faceted surfaces. This theory closely follows the LSW theory of Ostwald ripening in two-phase systems [1, 2, 3], but the mechanism of coarsening in faceted surfaces requires the addition of convolution terms recalling the work of Smoluchowski [4] and Schumann [5] on coalescence, and results in a novel coupling between the convolution and the rate of facet loss. As a generic framework, the theory concisely illustrates how the universal processes of facet removal and neighbor merger are moderated by the system-specific mean-field velocity describing average rates of length change. For a simple, example facet dynamics associated with the directional solidification of a binary alloy, agreement between predicted scaling state and that observed after direct numerical simulation of 40,000,000 facets is reasonable given the limiting assumption of non-correlation between neighbors; relaxing this assumption is a clear path forward toward improved quantitative agreement with data in the future.

1 Introduction

In many examples of faceted surface evolution, a *facet velocity law* giving the normal velocity of each facet can be observed, assumed, or derived. Examples of such dynamic laws describe growth of polycrystalline diamond films from the vapor [6, 7], evolution of faceted boundaries between two elastic solids [8], the evaporation/condensation mechanism of thermal annealing [9], and various solidification systems [10, 11, 12, 13, 14]. Such velocity laws are typically configurational, depending on surface properties of the facet such as area, perimeter, orientation, or position, and reduce the computational complexity of evolving a continuous surface to the level of a finite-dimensional system of ordinary differential equations. This theoretical simplification enables and invites large numerical simulations for the study of statistical behavior. This has been done frequently for one-dimensional surfaces [10, 11, 12, 13, 14, 15, 16, 17, 18, 19], while less frequently for two-dimensional surfaces due to the necessity of handling complicated topological events [9, 20, 21, 22, 23, 24]. Such inquiries reveal that many of the systems listed above exhibit coarsening – the continual vanishing of small facets and the increase in the average length of those that remain. Notably, these systems also display *dynamic scaling*, in which common geometric surface properties approach a constant statistical state, which is preserved even as the length scale increases.

The dynamic scaling behavior of coarsening faceted surfaces recalls the process of Ostwald ripening [25], in which small solid-phase grains in a liquid matrix dissolve, while larger grains accrete the resulting solute and grow in a scale-invariant way at late times. Indeed, it was observed some time ago that facets of alternating orientations on a one-dimensional surface are analogous to alternating phases of a separating two-phase alloy [26, 27], and the Cahn-Hilliard equation [28] which models phase separation has been used, in modified form, to describe several different kinds of faceted surface evolution [29, 30, 14]. More distantly related coarsening systems exhibiting dynamic scaling include coarsening cellular networks describing soap froths and polycrystalline films [31, 32, 33, 34, 35], and films growing via spiral defect [36]. In all of these cases, the system is characterized by a network of evolving boundaries which separate domains of possibly differing composition, and exhibit coarsening and convergence toward scale-invariant steady states.

Since dynamic scaling pushes complex systems into a state which can be approximately characterized by just a few statistics, it is natural to seek simplified models which approximately mimic the resulting scaling laws and scaling functions. The canonical example of this approach is the celebrated theory of Lifshitz, Slyozov, and Wagner describing Ostwald ripening [1, 2, 3]. Generically, such an approach selects a

distribution of some quantity, and includes just enough of the total system behavior to specify the effective behavior of that quantity – for example, the original LSW theory first identifies the average behavior of particles as a function of size, and uses that result to identify a continuity equation describing distribution evolution. Ideas of this kind have been applied to several of the higher-order cellular systems introduced above – for soap froths [37, 38], polycrystals [39], and spiral-growth films [36]. To the extent that such approaches mirror experimental data, they can yield valuable physical insight which cannot be gained by considering single particles, nor even by direct numerical simulation of larger ensembles. However, to date no similar attempt has been made for evolving faceted interfaces, which is somewhat surprising given the wide variety of examples of purely faceted motion, and past success in applying mean-field analyses to coarsening these systems.

In this work, therefore, we take a first step in that direction by introducing a framework for describing the distribution of facet lengths in 1D faceted surface evolution. Our approach closely resembles the LSW theory of Ostwald ripening, in that a number density $n(l, t)$, of facets of length l at time t, is transported by a known length-dependent effective velocity law. However, whereas vanishing drops in Ostwald ripening simply exit the system, each vanishing facet on a coarsening surface causes its two immediate neighbors to join together. Accounting for this process of merging requires the consideration of a convolution integral reminiscent of equations due to Smoluchowski [4] and Schumann [5] describing coagulation (see also Menon [40]). But since the removal rate of small facets from the system necessarily sets the rate of the concomitant merger of those neighboring facets, a particularly novel non-local coupling arises wherein the probability-flux at the origin is found to weight the convolution integral. We therefore arrive at the resulting novel evolution equation for the probability distribution $\rho(l, t)$ of facets of length l at time t to be

$$\frac{\partial \rho}{\partial t} + \frac{\partial}{\partial l}[\rho v] = -\rho(0, t) v(0, t) \int_0^l \rho(l - s, t) \rho(s, t) \, \mathrm{d}s, \tag{1}$$

where the *velocity*, $v(l, t)$, takes the special form

$$v(l, t) = \widehat{\mathcal{V}}[l, L(t)] \quad \text{with} \quad L(t) := \int_0^\infty l\rho(l, t)\mathrm{d}l \tag{2}$$

for a derived and prescribed *mean-field velocity* law, $\widehat{\mathcal{V}}(l, L)$, which encodes *an effective rate-of-change of length* for facets of length l purely in terms of that length, l, and the mean facet length L. The left hand side of Equation 1, and in particular the appearance there of the mean-field velocity $\widehat{\mathcal{V}}(l, L)$, is precisely where our theory mimics the essential transport concept underlying the LSW theory. In contrast, the convolution on the right hand side of 1 is strongly reminiscent of coagulation models Last, we note that the time-dependent function multiplying the convolution, $(\rho * \rho)$,

$$\mathcal{R} = -\rho(0, t) v(0, t),$$

is a rate of probability flux at the origin, which encodes the link between facets shrinking to zero and the concomitant merger of the two neighboring facets.

2 An Example Problem: From Modeling to Morphometrics

2.1 An Example Coarsening Dynamical System

During the directional solidification of a strongly anisotropic binary alloy, small-wavelength faceted surfaces develop. If the alloy is solidified above a critical velocity, a layer of supercooled liquid is created at the interface, which drives a coarsening instability governed by the facet dynamics [14]

$$\mathcal{V}_i = \cos(\omega) \, h_i, \tag{3}$$

where $\mathcal{V}_i$, $(-1)^i \omega$ and h_i are the (instantaneous) normal velocity, fixed facet angle (the **Wulff angle**) and mean height of the ith facet respectively. Letting $l_i(t)$ denote the length of the ith facet at time t, we will now
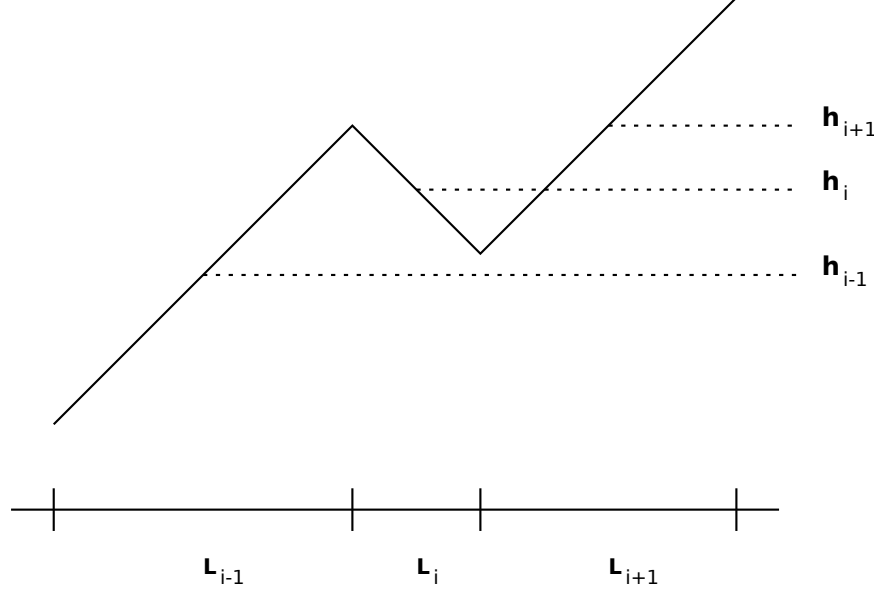
Figure 1: A diagram illustrating a representative facet and its two neighbors. Here h_i denotes the *mean height* of the center facet, while L_i denotes its width (length). Similarly for the neighbors of the center facet.

show that, between coarsening events, one can derive from Equation 3 a dynamical system for these facet lengths. First, we note the general, *kinematic* relation

$$\frac{\mathrm{d}l_i}{\mathrm{d}t} = \frac{(-1)^i}{\sin(2\omega)} (\mathcal{V}_{i+1} - \mathcal{V}_{i-1}) ; \tag{4}$$

the prefactor $(-1)^i$ reflects our convention that odd (even) facets have negative (positive) slopes. If we now use the facet velocity law (3) to specify the *dynamics*, we can convert this equation, via elementary geometry (see Figure 1), to a dynamical system on facet lengths alone:

$$\frac{dl_i}{dt} = \frac{1}{4} (2l_i - l_{i+1} - l_{i-1}) . \tag{5}$$

Thus, even though the normal velocity of a facet depends on its mean height and slope, the rate of change of its length does not.

Now the morphometric structure of the evolving coarsening faceted surface is encoded in an ordered facet-length ensemble, denoted $\mathcal{L}[t] : \mathbb{Z} \to (0, \infty)$, associated with the evolving interface; $\mathcal{L}[t](i) := l_i(t)$. Since the dynamical system (5) results in lengths which tend to zero, resulting in the merging of the two neighboring facets (a coarsening event), we need to *re-write* $\mathcal{L}[t]$ at such critical times. To see how, we again consider Figure 1, and imagine that the jth facet F_j shrinks to length 0 at the critical time t^*. When this happens, this F_j obviously vanishes; but in addition, the two neighbors of F_j, namely F_{j-1} and F_{j+1} also vanish as independent entities, to be replaced by a new facet with length equal to the sum of the lengths of its ancestors. A natural re-indexing of the resultant faceted surface provides the following *update rule* $\mathcal{L}[t_*^+]$

$$\mathcal{L}[t_*^+](i) := \begin{cases} \mathcal{L}[t_*^-](i+1) & i \le j-2, \\ \mathcal{L}[t_*^-](j-1) + \mathcal{L}[t_*^-](j+1) & i = j, \\ \mathcal{L}[t_*^-](i-1) & i \ge j+2. \end{cases} \tag{6}$$

Taken together, 5 and 6 constitute a *Coarsening Dynamical System* (CDS), which is the object of our further study.

2.2 Numerical Simulation and Morphological Statistics

For three different initial length distributions, random faceted surfaces containing 1,000,000 facets were constructed by generating two sets of numbers obeying that distribution, and scaled to have equal sums; these random lengths were then interleaved to generate a periodic faceted surface. The initial empirical distributions of facet lengths $\varrho(l)$ were

$$\begin{aligned}
\varrho_{0,\text{comp.}}(l) &= \frac{10}{18}\chi_{\left(\frac{1}{10},\frac{19}{10}\right)} \\
\varrho_{0,\text{exp.}}(l) &= \exp(-l) \\
\varrho_{0,\text{poly.}}(l) &= \frac{2}{(1+l)^3}
\end{aligned} \qquad . \tag{7}$$

Hence, we have explored initial distributions of facet lengths with compact support, exponential decay, and polynomial decay.

Figure 2.2a depicts a representative local patch of surface evolving under the CDS (5),(6). There, the locations of facet boundaries (corners) are plotted over time, and we see many instances of the binary coarsening described by the update rule 6. As the system continues to evolve, all three initial conditions begin to coarsen exponentially, with the average facet length $L(t) \propto e^{1.8t}$ at late times (Figure 2.2b). The arrival at this rate indicates the attainment of the *scaling state*, in which the associated empirical probability distribution $\varrho(l,t)$, of facet lengths l at time t, is observed to approach a universal scale-invariant form

$$\varrho(l,t) \xrightarrow{t\to+\infty} \frac{1}{\langle\mathcal{L}(t)\rangle}\mathfrak{P}\left(\frac{l}{\langle\mathcal{L}(t)\rangle}\right). \tag{8}$$

which is illustrated in Figure 2.2c.

3 A Mean-Field Theory for Binary-Coarsening Faceted Surfaces

We now turn to a theoretical study of the evolving facet ensemble associated with the CDS. Our focus is the formulation of a general theory which sheds light on the empirical probability distribution $\varrho(l,t)$. Inspired by LSW theory, our aim is to formulate an approximation for ϱ by rationally constructing a mass-transport evolution equation for a theoretical probability function $\rho(l,t)$, supplemented by sinks/sources which simultaneously and properly account for the appropriate coarsening mechanism of the original CDS. Our closed theory emerges from a number of mean-field approximations of the underlying facet ensemble; such approximations are often referred to as *mean-field hypothesis*.

3.1 Preliminaries

We begin by introducing a number of quantities derived from $\rho(l,t)$ that are specific to coarsening systems. First, as small facets shrink to zero and are removed from the system, the *average length* $L(t)$ of the remaining facets increases. This monotonically-increasing quantity is simply the first moment of ρ:

$$L(t) := \int_0^\infty l\rho(l,t)\,\mathrm{d}l.$$

Second, we define the *number density* per unit length, $n(l,t)$, by

$$n(l,t) := \frac{1}{L(t)}\rho(l,t); \tag{9}$$

Note that the zeroeth moment $N(t) = \int n(l,t)\,\mathrm{d}l$ - which counts the total number of facets - decreases as $L(t)$ increases. However, its first moment $\int l\,n(l,t)\,\mathrm{d}l \equiv 1$ is a conserved quantity, reflecting the fact that the conserved quantity in our coarsening faceted surface is the total interface length.
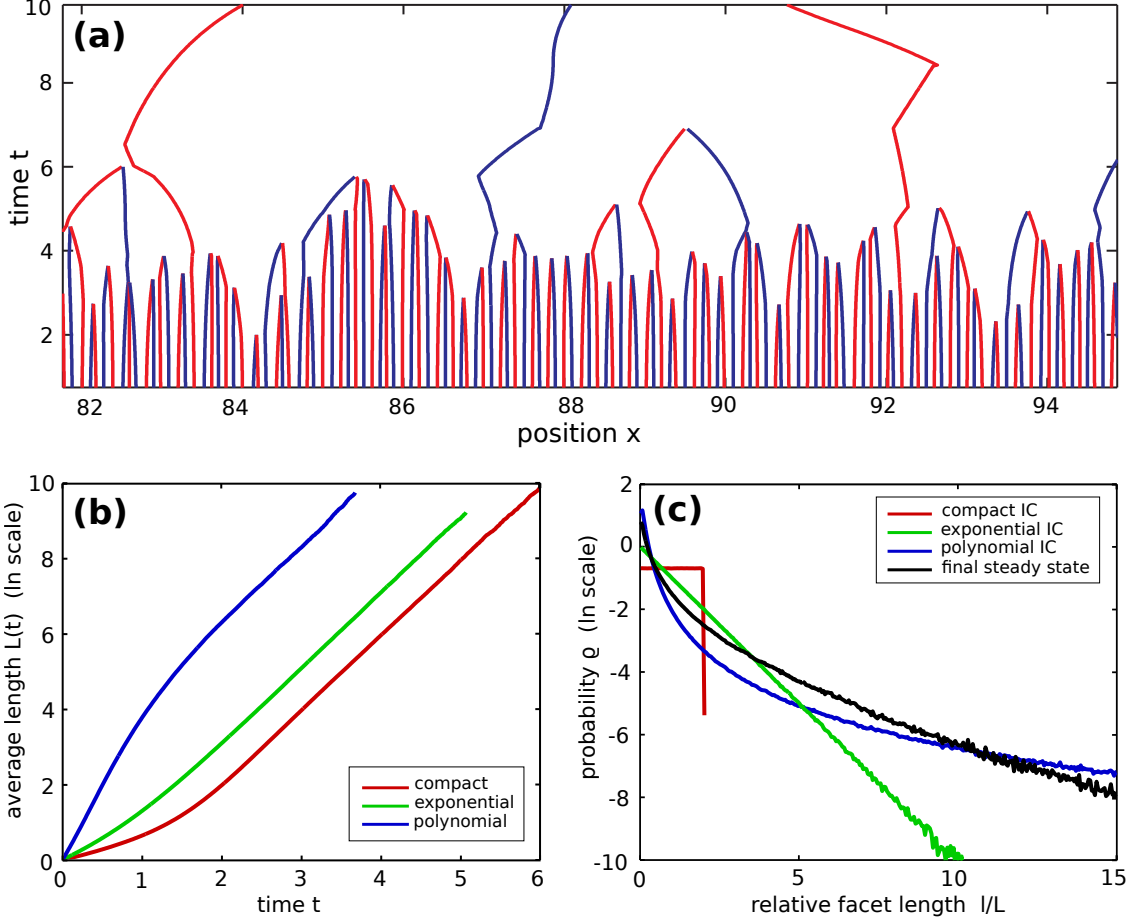
4

Figure 2: Survey of coarsening behavior. (a) A representative example of the evolution of corners between facets (red/blue correspond to hills/valleys). (b) Facet length scale growth with time for each of the initial conditions (7) (natural log scale). (c) Numerically observed scaling function $\mathfrak{P}\left(\frac{l}{\langle \mathcal{L}(t) \rangle}\right)$, compared against each of the initial conditions (7) (natural log scale).

Finally, we presume that under a *closure* or *mean-field hypothesis* of statistically independent neighboring facet lengths, it is possible to formulate a probabilistic, length-dependent *transport rate*

$$v\left(l,t\right) := \left\langle \frac{dl}{dt} \right\rangle \left(l,t\right). \tag{10}$$

describing the average rate of length change for facets of length l at time t.

3.2 Derivation of an Evolution Equation

The existence of $v\left(l,t\right)$ implies a *population flux* $J\left(l,t\right)$

$$J(l,t) := n(l,t)\, v(l,t). \tag{11}$$

For a generic *coarsening* system, $v\left(l,t\right) < 0$ in some neighborhood of $l = 0$; the rate of facet removal is then given by the population flux into the origin

$$R\left(t\right) := -J\left(0,t\right) > 0. \tag{12}$$

5

Under the coarsening rule (6), these facets are removed from the population, as are the two neighboring facets; the latter are then replaced with a new facet with length equal to the sum of the neighbor lengths:

$$(\cdots, \mathcal{L}^-, \mathcal{L}, \mathcal{L}^+, \cdots) \xrightarrow{\mathcal{L} \to 0^+} (\cdots, \mathcal{L}^- + \mathcal{L}^+, \cdots).$$

According to our closure hypothesis, the two lost neighbors $\mathcal{L}^-$ and $\mathcal{L}^+$ are each independently distributed according to the probability distribution $\rho(l, t)$. Therefore, the facet $\mathcal{L}^- + \mathcal{L}^+$ which replaces them, being the sum of two random variables, satisfies the *joint probability function*

$$[\rho * \rho](l, t) = \int_0^l \rho(s, t)\rho(l - s, t)\, \mathrm{d}s \tag{13}$$

Hence, the coarsening process, in addition to transporting particles out of the domain at $l = 0$ at a rate of R, induces both a loss L_C and a gain G_C of particles with length l at rates

$$L_C(l, t) = 2R(t)\rho(l, t) \tag{14}$$
$$G_C(l, t) = R(t)[\rho * \rho](l, t). \tag{15}$$

Taken together, the population flux (11), the neighbor-loss rate (14), and the neighbor-replacement rate (15) imply a balance law on the number density given by

$$\frac{\partial n}{\partial t} + \frac{\partial}{\partial l}(nv) = R(\rho * \rho - 2\rho). \tag{16}$$

We now proceed to recast the left-hand side of Eqn. (16) purely in terms of the probability density ρ. To that end, it will be useful to introduce the *probability flux*, $\mathcal{J}$,

$$\mathcal{J}(l, t) := \rho(l, t)\, v(l, t) = L(t)\, J(l, t)$$

and the associated probability flux at the origin, (rate of flux of probability at 0)

$$\mathcal{R}(t) := \mathcal{J}(0, t) = L(t)R(t).$$

Noting that integrating the number density (16) with respect to l over the interval $(0, \infty)$ yields a rate of facet loss $\frac{\mathrm{d}N}{\mathrm{d}t}$ given by

$$\frac{\mathrm{d}N}{\mathrm{d}t} = \frac{\mathrm{d}}{\mathrm{d}t}\left(\frac{1}{L}\right) = -2R = -2\frac{\mathcal{R}}{L}, \tag{17}$$

we obtain

$$\frac{\partial n}{\partial t} = \frac{\partial}{\partial t}\left(\frac{\rho}{L}\right) = -2\frac{\mathcal{R}}{L}\rho + \frac{1}{L}\frac{\partial \rho}{\partial t}. \tag{18}$$

Inserting (18) into (16), we conclude that the governing equation for the probability distribution $\rho(l, t)$ is

$$\boxed{\rho_t + (\rho v)_l = \mathcal{R}(\rho * \rho)}. \tag{19}$$

This equation - our main result - is generic to coarsening faceted surfaces exhibiting binary coarsening, with the effect of the particular facet dynamics limited to the term $v(l, t)$.

3.3 Predictions: Growth Rate and Scaling State

To investigate the scaling state of Equations (19) and (24), we make the *scaling hypothesis* that

$$\rho(l, t) = \frac{1}{L(t)}\mathcal{P}\left(\frac{l}{L(t)}\right) \tag{20}$$

where

$$\int_0^\infty \mathcal{P}(l)\, \mathrm{d}l = 1 \quad \text{and} \quad \int_0^\infty l\,\mathcal{P}(l)\, \mathrm{d}l = 1. \tag{21}$$

This hypothesis leads to two main results. First, recalling (17) and (12), we obtain a differential equation on $L(t)$:

$$\frac{\mathrm{d}}{\mathrm{d}t}\left(\frac{1}{L}\right) = -2\left[n(0,t)\,v(0,t)\right] = -\frac{\mathcal{P}(0)}{L}.$$

Hence, the theory predicts that the average facet length grows according to to the exponential relation

$$L(t) = \exp\left[\mathcal{P}(0)\,t\right];\tag{22}$$

this form is independent of the particular facet dynamics, which serve only to choose the constant $\mathcal{P}(0)$. Second, upon inserting the ansatz (20) into (19), we obtain for the *scaling function* $\mathcal{P}(x)$ the governing equation

$$\frac{\mathrm{d}}{\mathrm{d}x}\left[v(x)\,\mathcal{P}(x)\right] = \mathcal{P}(0)\left\{\int_0^\infty \mathcal{P}(x)\,\mathcal{P}(\xi - x)\,\mathrm{d}\xi + 2\frac{\mathrm{d}}{\mathrm{d}x}\left(x\mathcal{P}(x)\right)\right\};\tag{23}$$

this integro-differential equation implicitly defines $\mathcal{P}(x)$, and can be solved at least numerically. The results (22) and (23) are the central predictions of our theory.

4 Comparison of Theory vs Data for our Example Dynamics

We now apply the generic theory of Section 3 to the specific example dynamics (5) from Section 2, and compare the theoretical predictions on ρ with the empirical statistical data ϱ.

Application of the general theory   To generate a theory specific to the dynamics (3), all that is required is to calculate the mean-field velocity $v(l,t)$ associated with the dynamics (5), and insert it into the relevant generic equations of section 3. From (5), the application of our neighbor-independence hypothesis leads immediately to

$$v(l,t) = \frac{1}{2}\left(l - L(t)\right).\tag{24}$$

Inserting (24) into the generic scaling state equation (23) yields as the definition of the scaling function for this dynamics the equation

$$\frac{\mathrm{d}}{\mathrm{d}x}\left[(x-1)\,\mathcal{P}(x)\right] = 2\mathcal{P}(0)\left\{\int_0^\infty \mathcal{P}(x)\,\mathcal{P}(\xi - x)\,\mathrm{d}\xi + 2\frac{\mathrm{d}}{\mathrm{d}x}\left(x\mathcal{P}(x)\right)\right\}.\tag{25}$$

By inspection, a solution to this equation happens to be

$$\mathcal{P}(x) = \exp(-x),\tag{26}$$

and hence, the average facet length is predicted to grow at late times as

$$L(t) = e^{\mathcal{P}(0)t} = e^t.\tag{27}$$

Comparison with Data   We now compare the predictions (22) and (26) against steady state statistics obtained via direct simulation of the dynamics (3). First, the observed statistical coarsening rate of $e^{1.8t}$, although different from the predicted rate of e^t, is consistent with the generic prediction 22, in that our observed scaling state exhibited $\mathfrak{P}(0) \approx 1.8$. This is unsurprising, because the prediction 22 is obtained ultimately from the conservation of total surface length. The discrepancy between actual values is due to a difference in the scaling state itself, shown in Figure 4. There the predicted exponential distribution is shown in blue; comparison with the observed distribution (green) reveals qualitative but not quantitative agreement. In particular, although both distributions exhibit exponential decay in the dimensionless relative length l/L, the observed distribution has more of its mass near zero and in the tail, which decays like $\exp\left(-\frac{x}{2}\right)$ rather than the predicted $\exp(-x)$.

Diagnostic Tests for the source of disagreement   Seeking the cause of quantitative discrepancies between theory and experiment, we re-examine the two main assumptions used to construct the theory: the existence of a statistical mean field velocity, and the non-correlation of neighboring facet lengths.
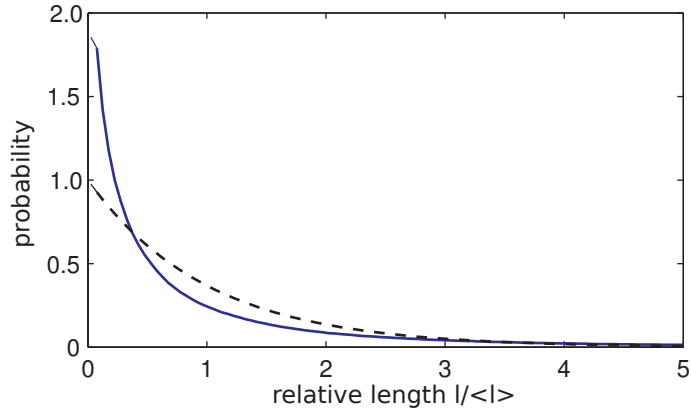
Figure 3: Comparison between the theoretically-predicted scaling function $\mathcal{P}(x)$ (blue) and the empirically-observed function $\mathfrak{P}(x)$ (black dashes).
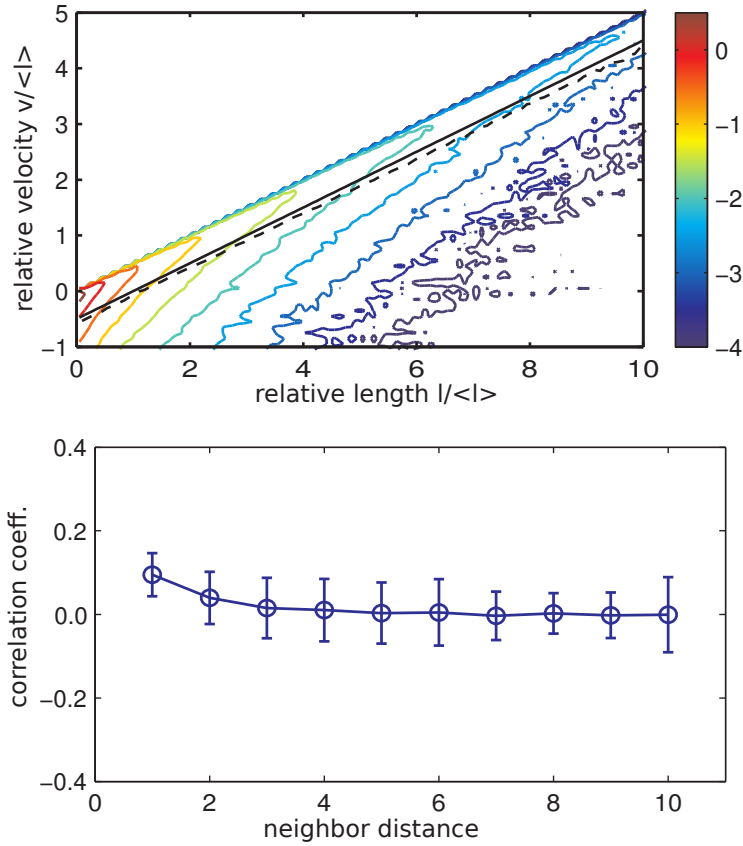

Figure 4: Diagnostic tests: (a) Contour of the logarithm of the statistical distribution of dimensionless length/velocity pairs $\varrho(\frac{l}{L}, \frac{v}{L})$. The mean statistical velocity (obtained by integrating in $\frac{v}{L}$) is plotted as a dotted line, while the predicted velocity $v\left(\frac{l}{L}\right)$ is a solid line. (b) Steady-state correlation of facet lengths as a function of neighbor distance d. Plotted is the correlation coefficient of all length pairs $\left(l_i, l_{(i+d)\%n}\right)$.

8

Mean-field velocity. To test the validity of the assumption of an effective flux function $v(l)$, we construct a two-point distribution of length/velocity pairs (l, v) as they occur in the simulated ensembles. A contour plot of the logarithm of this distribution is shown in Figure 4. Finding the mean velocity for each length gives the statistical v (dashes), which turns out to compare favorably with the predicted v (solid). A slight shift between the curves is observed, which we attribute to a discretization error associated with binning our sample data into boxes of width 0.1 in the relative velocity and relative lengths. So this approximation seems to be reasonable.

Non-correlation. To test the validity of the assumption of non-correlation between neighboring facets, we measure the correlation coefficient of each nth-neighbor pair for various n. These coefficients tend toward a steady state as the ensembles evolve, and that state is shown in figure Figure 4b. There we see a small but possibly significant positive correlation for at least the first two neighbors, suggesting that facets of similar size tend to cluster together - large with large, and small with small. Hence, the non-correlation assumption fails, though not spectacularly. This result is not surprising, as the main weakness of the original LSW theory which inspires this work was also a failure to address correlations; later generalizations which corrected this deficiency agreed well with experimental data [41].

5   Conclusions

We have presented a mean-field theory for the evolution of length distributions associated with coarsening faceted surfaces. In the spirit of LSW theory, a facet-velocity law governing surface evolution is used to establish a characteristic length-change law; this *mean-field velocity*, along with a consideration of the effect of binary coarsening events observed during simulation, leads to a novel continuity equation governing the evolution of the probability distribution. This equation combines a transport term similar to LSW theory with a convolution term reminiscent of coagulation-fragmentation models. However, it is novel in that the latter process occurs at a rate determined by the magnitude of transport at the boundary. Our model therefore serves, apart from the direct application to facet dynamics, as a study of a new class of mean-field equation.

For a sample facet dynamics associated with binary solidification, we find the growth rate, scaling state, and coarsening efficiency predicted by our framework, and then compare the predictions to statistics obtained from direct numerical simulation of a large facet ensemble. The results, although not quantitative, agree surprisingly well for a single-point statistic. In addition, the theory captures the essential feature of the dynamically scaling state – a particular mass flux law which drives coarsening by pushing facets away from the average length, moderated by competing terms describing coarsening and continuous rescaling, which push mass toward infinity and zero, respectively. While later improvements to our model addressing neighbor correlation will undoubtedly increase its predictive capabilities, these same forces will still balance in the steady state. The model as presented thus serves as a qualitative explanation of the essential features of the scaling state, as well as a guide to further research efforts.

References

[1] I. M. Lifshitz and V. V. Slezov. Kinetics of diffusive decomposition of supersaturated solid solutions. *Soviet Physics JETP*, 38:331–339, 1959.

[2] I.M Lifshitz and V. V. Slyozov. The kinetics of precipitation from supersaturated solid solutions. *Journal of Physics and Chemistry of Solids*, 19:35–50, 1961.

[3] Carl Wagner. Theorie der alterung von niederschlägen durch umlösen. *Zeitschrift für Elektrochemie*, 65:581–591, 1961.

[4] M. von Smoluchowski. Drei vorträge über diffusion, brownsche molekularbewegung und koagulation von kolloidteilchen. *Physikalische Zeitschrift*, 17:557–571, 1916.

[5] T. E.W. Schumann. Theoretical aspects of the size distribution of fog particles. *Quarterly Journal of the Royal Meteorological Society*, 66:195–207, 1940.

[6] A. N. Kolmogorov. To the "geometric selection" of crystals. *Dokl. Acad. Nauk. USSR*, 65:681–684, 1940.

[7] A. van der Drift. Evolutionary selection, a principle governing growth orientation in vapor-deposited layers. *Philips Research Reports*, 22:267–288, 1967.

[8] M. E. Gurtin and P. W. Voorhees. On the effects of elastic stress on the motion of fully faceted interfaces. *Acta Materialia*, 46(6):2103–2112, 1998.

[9] S. J. Watson and S. A. Norris. Scaling theory and morphometrics for a coarsening multiscale surface, via a principle of maximal dissipation. *Phys. Rev. Lett.*, 96:176103, 2006.

[10] L. Pfeiffer, S. Paine, G. H. Gilmer, W. van Saarloos, and K. W. West. Pattern formation resulting from faceted growth in zone-melted thin films. *Phys. Rev. Lett.*, 54(17):1944–1947, 1985.

[11] D. K. Shangguan and J. D. Hunt. Dynamical study of the pattern formation of faceted cellular array growth. *Journal of Crystal Growth*, 96:856–870, 1989.

[12] C. L. Emmot and A. J. Bray. Coarsening dynamics of a one-dimensional driven Cahn-Hilliard system. *Phys. Rev. E*, 54(5):4568–4575, 1996.

[13] S. J. Watson, F. Otto, B. Y. Rubinstein, and S. H. Davis. Coarsening dynamics of the convective Cahn-Hilliard equation. *Physica D*, 178(3-4):127–148, April 2003.

[14] S. A. Norris, S. H. Davis, P. W. Voorhees, and S. J. Watson. Faceted interfaces in directional solidification. *Journal of Crystal Growth*, 310:414–427, 2008.

[15] C. Wild, N. Herres, and P. Koidl. Texture formation in polycrystalline diamond films. *J. Appl. Phys.*, 68(3):973–978, 1990.

[16] J. M. Thijssen, H. J.F. Knops, and A. J. Dammers. Dynamic scaling in polycrystalline growth. *Phys. Rev. B*, 45(15):8650–8656, 1992.

[17] Paritosh, D. J. Srolovitz, C. C. Battaile, and J. E. Butler. Simulation of faceted film growth in two dimensions: Microstructure, morphology, and texture. *Acta Materialia*, 47(7):2269–2281, 1999.

[18] J. Zhang and J. B. Adams. FACET: a novel model of simulation and visualization of polycrystalline thin film growth. *Modeling Simul. Mater. Sci. Eng*, 10:381–401, 2002.

[19] J. Zhang and J. B. Adams. Modeling and visualization of polycrystalline thin film growth. *Computational Materials Science*, 31(3-4):317–328, November 2004.

[20] J. M. Thijssen. Simulations of polycrystalline growth in 2+1 dimensions. *Phys. Rev. B*, 51(3):1985–1988, 1995.

[21] S. Barrat, P. Pigeat, and E. Bauer-Grosse. Three-dimensional simulation of CVD diamond film growth. *Diamond and Related Materials*, 5:276–280, 1996.

[22] G. Russo and P. Smereka. A level-set method for the evolution of faceted crystals. *SIAM Journal of Scientific Computing*, 21(6):2073–2095, 2000.

[23] P. Smereka, X. Li, G. Russo, and D. J. Srolovitz. Simulation of faceted film growth in three dimensions: Microstructure, morphology, and texture. *Acta Materialia*, 53:1191–1204, 2005.

[24] S. A. Norris and S. J. Watson. Geometric simulation and surface statistics of coarsening faceted surfaces. *Acta Materialia*, 55:6444–6452, 2007.

[25] W. Ostwald. *Z. Phys. Chem.*, 34:495, 1900.

[26] W. W. Mullins. Theory of linear facet growth during thermal etching. *Philosophical Magazine*, 6(71):1313–1341, November 1961.

[27] N. Cabrera. On stability of structure of crystal surfaces. In *Symposium on Properties of Surfaces*, ASTM Materials Science Series – 4, pages 24–31, 1916 Race St., Philadelphia, PA, 1963. American Society for Testing and Materials, American Society for Testing and Materials.

[28] J. W. Cahn and J. E. Hilliard. Free energy of a nonuniform system. I. Interfacial free energy. *J. Chem Phys*, 28:258, 1958.

[29] F. Liu and H. Metiu. Dynamics of phase separation of crystal surfaces. *Phys. Rev. B*, 48(9):5808–5818, September 1993.

[30] A. A. Golovin, S. H. Davis, and A. A. Nepomnyashchy. A convective Cahn-Hilliard model for the formation of facets and corners in crystal growth. *Physica D*, 122:202–230, 1998.

[31] J. Stavans. The evolution of cellular structures. *Reports on Progress in Physics*, 56(6):733–789, June 1993.

[32] V. E. Fradkov and D. Udler. Two-dimensional normal grain growth: Topological aspects. *Advances in Physics*, 43(6):739–789, 1994.

[33] H. J. Frost and C. V. Thompson. Computer simulation of grain growth. *Current Opinion in Solid State and Materials Science*, 1(3):361–368, 1996.

[34] C. V. Thompson. Grain growth and evolution of other cellular structures. *Solid State Physics*, 55:269–314, 2001.

[35] G. Schliecker. Structure and dynamics of cellular systems. *Advances in Physics*, 51(5):1319–1378, 2002.

[36] T. P. Schulze and R. V. Kohn. A geometric model for coarsening during spiral-mode growth of thin films. *Physica D*, 132:520–542, 1999.

[37] C. W.J. Beenakker. Evolution of two-dimensional soap-film networks. *Phys. Rev. Lett.*, 57(19):2454–2457, 1986.

[38] H. Flyvbjerg. Model for coarsening froths and foams. *Phys. Rev. E*, 47(6):4037–4054, June 1993.

[39] Katayun Barmak, Eva Eggeling, Maria Emelianenko, Yekaterina Epshteyn, David Kinderlehrer, Richard Sharp, and Shlomo Ta'asan. An entropy-based theory of the grain boundary character distribution. *Discrete and Continuous Dynamical Systems - Series A*, 30:427–454, 2011.

[40] G. Menon, B. Niethammer, and R. L. Pego. Dynamics and self-similarity in min-driven clustering. *Transaction of the American Mathematical Society*, 362:6591–6618, 2010.

[41] M. Marder. Correlations and ostwald ripening. *Phys. Rev. A*, 36(2):858–874, 1987.